International Journal of Greenhouse Gas Control 132 (2024) 104073

Contents lists available at ScienceDirect

International Journal of Greenhouse Gas Control

journal homepage: www.elsevier.com/locate/ijggc

Nanoscale mechanical properties of organic-rich Draupne caprock shale using nano-indentation method, offshore Norway

Md Jamilur Rahman [a,*], Maxim Lebedev [b], Nazmul Haque Mondol [a,c]

[a] Department of Geosciences, University of Oslo (UiO), Sem Sælands vei 1 0371, Oslo, Norway
[b] Curtin University (CU), Kent Street, Bentley 6102, Perth, Western, Australia
[c] Norwegian Geotechnical Institute (NGI), Sognsveien 72 0806, Oslo, Norway

ARTICLE INFO

Keywords:
Nanoscale
Organic-rich shale
Mechanical property
Offshore norway
Draupne shale
CO_2 sequestration

ABSTRACT

Mechanical properties of cap and overburden rocks are crucial for field-scale geomechanical modeling and simulation of subsurface CO_2 storage and hydrocarbon production. However, obtaining these properties can be challenging due to the lack of core extraction during drilling. The nano-indentation technique offers a solution to this problem by allowing the estimation of mechanical properties using small samples such as cuttings. This study evaluated 12 organic-rich shale samples from the North Sea to measure nanoscale mechanical properties. Half of these samples were cuttings, allowing for a sensitivity analysis between core and cuttings samples. A comparative analysis of the nanoscale and triaxial lab tests has been conducted. It is found that the mineralogical composition significantly affected the mechanical properties, with a strong negative correlation observed between Young's modulus and brittle mineral assemblages. The sensitivity analysis demonstrated that properties estimated from cuttings were reliable, like those obtained from core samples. This study suggests that the nano-indentation technique is a practical and reliable method that can add significant values and reduce uncertainty in field-scale geomechanical simulation.

1. Introduction

Characterizing the mechanical properties of organic-rich shale for sealing potential is crucial for hydrocarbon exploitation and for the successful geological storage of fluids (i.e., CO_2, H_2, wastewater, etc.). Although the North Sea is a mature basin, many complex structures still need to be evaluated. In addition, the North Sea will be the future geological CO_2 storage (CCS) hub, which is already in progress with a plan to inject a gigatonnes level of CO_2 from 2024. Therefore, it is critical to evaluate the mechanical properties of primary and secondary (within overburden) caprocks within the area.

The primary caprock of the North Sea, the upper Jurassic organic-rich shales are mainly composed of fine-grained clay and silt-sized particles with a diverse range of thickness, porosity, mineralogy, and heterogeneity (Hart et al., 2013; Mondol et al., 2007; Mondol, 2018; Storvoll et al., 2005). Shales, in general, act as a top seal with having exceptionally high capillary entry pressure compared to the reservoir sandstones (Forschi and Cartwright, 2020; Hu et al., 2012; Mehmani et al., 2013; Zhang et al., 2015a; Schowalter, 1979) and extremely low permeability (Amann-Hildenbrand et al., 2012; Mondol et al., 2008; Sakhaee-Pour and Bryant, 2012; Zhang et al., 2015b, 2017) due to their low pore connectivity. As a result of these characteristics of shale, it is unlikely to have a capillary breakthrough within caprock shales. However, mechanical failure in caprock may occur when reservoir pore pressure exceeds the fracture strength due to hydrocarbon accumulation or any fluid injection (Ingram et al., 1997). The presence of gas chimneys worldwide indicated the possible hydrocarbon leakage through the top seal. The risk of failure might increase significantly in fluid injection sites due to increased injection-induced reservoir pressure. Hence, the mechanical properties of caprock in the North Sea are essential for successful hydrocarbon exploration and reliable subsurface geological storage of fluids.

The fracturing processes in organic-rich shales are complex and depend on various factors, such as shale's mineralogical compositions, brittleness, thickness, etc., which can be challenging to quantify (Sone and Zoback, 2013a, 2013b; Vernik and Milovac, 2011). The mechanical rock deformation behavior due to stress varied depending on the caprock shale ductility (Nygård et al., 2006). The ductility or brittleness of caprock is a complex property and can be estimated from rock strength properties such as Young's modulus and Poisson's ratio

* Corresponding author.
E-mail address: m.j.rahman@geo.uio.no (M.J. Rahman).

https://doi.org/10.1016/j.ijggc.2024.104073
Received 7 April 2023; Received in revised form 24 November 2023; Accepted 15 January 2024
Available online 20 January 2024

(Rickman et al., 2008). Moreover, core samples are usually required for estimating shale rock strength properties. These properties are typically estimated through expensive laboratory experiments, such as unconfined and confined triaxial compression and shear test (Colmenares and Zoback, 2002; Minaeian et al., 2014; Lama and Vutukuri, 1978), ultrasonic techniques (Wang, 2002), etc. In addition, fracture toughness can be determined from cracked chevron notched Brazilian disk (CCNBD), single edge notch beam (SENB), and three-point bending tests (Xiong et al., 2019; Zuo et al., 2019, 2020). However, these laboratory tests often require relatively large core samples, which may be challenging to obtain (Hongyan et al., 2013; Tianshou and Ping, 2014) and can also result in high inter-sample variability (Du et al., 2020; Li et al., 2020). Additionally, core samples are often acquired from the reservoir intervals during drilling, leaving limited samples available for the analysis of cap and overburden rocks. To address this data scarcity in caprock and overburden, seismic data inverted mechanical properties have been used to illustrate significant lateral and vertical heterogeneity (Fawad et al., 2021, 2020) and can be used in the 3D field-scale geomechanical simulation (Rahman et al., 2022a, 2022c). Although the inversion process solved the insufficient data issues, the inverted properties require to validate using lab measurements. However, despite the importance of laboratory investigation for any geomechanical assessment, due to the lack of core samples, there are not enough conventional laboratory measurements from the cap and overburden intervals. These data gaps within cap and overburden intervals motivate us to conduct this nanoscale property estimation study where the nano-indentation method has been implemented.

The application of the nano-indentation technique in geoscience was first proposed by Oliver and Pharr (2004, 1992) as a method to determine rock mechanical properties such as hardness (H), creep modulus (C), and indentation modulus (M) using small samples. The indentation depth generated by applying load to the rock samples can be used to estimate these properties. However, the maximum applied load can significantly influence the average properties by capturing the grain level modifications. Although this method can estimate several mechanical properties, no standardized indentation benchmark is still available for materials such as shales (Du et al., 2020). Because nano-indentation measurement requires a small sample compared to traditional laboratory measurements, it is now possible to estimate rock strength properties within caprock and overburden interval. As we lack cores within caprocks and almost no cores from overburden, this method can be crucial in subsurface fluid injection projects because we can use the cuttings to estimate rock properties. Considering the heterogeneity in overburden intervals and consequences in field-scale rock geomechanical behavior, we must evaluate the mechanical properties of the overburden rock intervals. Overbuden geomechanical characterization is required in fluid injection projects due to tracking the fluid plume even long after the injection period. Nano-indentation method can be the solution for data scarcity issues in field-scale geomechanical simulation.

In this research, we evaluated the mechanical properties of organic-rich Draupne caprock shales using the nano-indention method. The effectiveness of cutting samples as input for lab experiments was tested by comparing the results obtained from the core and cutting samples from the same well. Also, the nanoscale results and conventional laboratory experiment databases were compared to validate the properties obtained at the nanoscale. Furthermore, the sensitivity of the maximum load was investigated using available mineralogical and petrographic databases. However, it should be noted that this study does not consider the effect of lamination on the estimated results, though the caprock shale is highly anisotropic. Results from this study might open a window for having a rock mechanical property database within the overburden section where very minimal or no cores are present but critical in geomechanical simulation.

2. Experimental methods

2.1. Experiment apparatus and specimens

In this study, an IBIS nano-indentation system from Fischer-Cripps Laboratories was employed to measure the nanoscale properties of the samples. The '*grid indentation*' method, was utilized, which involves a series of evenly distributed square lattices on the surface of the specimen, using a Berkovich indenter (Fig. 1). The applied load on the indenter could vary between 1 mN to 500 mN, with a load and depth resolution of 0.07 μN and 0.003 nm, respectively. Both core and cutting samples were attached to a rigid substrate, then polished to achieve a flat surface with an average roughness of 0.01 μm, and placed inside the nano-indenter. A maximum load of 10 mN was used in sample loading-unloading cycles; however, a load of 100 mN was applied to a few samples to evaluate the load sensitivity on the rock modulus.

Twelve samples were collected from six wells (i.e., 15/3–8, 15/12–21, 32/2–1, 32/4–1, 34/4–3 & 35/11–4) in the North Sea, especially from the organic-rich Draupne caprock shale formation. These samples were used to evaluate the caprock shale's nanoscale mechanical properties, such as hardness and indentation modulus. The samples were taken from depths ranging from 502 m to 4317 m, present-day depth below the seafloor (BSF). The paleo-temperature data (corrected for exhumation) suggests that the samples cover both mechanical compaction (MC) and chemical compaction (CC) regions, with the transition depth being around 60–70 °C. Half of the samples were cuttings. A sensitivity analysis was conducted to compare the results obtained from core and cuttings samples using the data from well 15/3–8. Also, note that only the vertical surface of the core and cutting samples have been indented, as most of the cutting samples do not have horizontal faces.

2.2. Hardness and indentation modulus

The nano-indentation experiment is used to estimate the hardness and indentation modulus of the Draupne caprock shales by extracting information from the load-displacement curves (Fig. 1). The nanoscale hardness (H) is calculated by taking the ratio of maximum indentation load (P_{max}) to the projected area of contact (A_c) using the following equation:

$$H = \frac{P_{max}}{A_c}, \tag{1}$$

The maximum load (P_{max}) used in this study is 10 & 100 mN, and the area of contact (A_c) is calculated using the contact depth (h_c). In this study, a Berkovich indenter is used for the nano-indentation measurements. The area of contact of a Berkovich indenter can be estimated by the function of the contact depth (h_c).

$$A_c = 24.5h_c^2, \tag{2}$$

The parameter h_c is the elastic displacement during unloading (Fig. 1b) be related to the maximum indentation depth (h_{max}) and the applied load (P_{max}). The relationship between h_c and other parameters are estimated using the following equation.

$$h_c/h_{max} = 1 - \varepsilon P_{max}/(Sh_{max}), \tag{3}$$

Where the constant ε is related to the geometry of the indenter, it is equal to 0.75 for a Berkovich indenter. The contact stiffness (S) is used to assess the derivative at P_{max} and can be estimated by differentiating the fitting F-h function of the unloading curve. Mathematically it can be expressed as follows:

$$S = \frac{\delta F}{\delta h}|_{h_{max}} \tag{4}$$

The Bulychev-alekhin-shoroshorov (BASh) equation (Bulychev et al., 1975) can be used to quantify the yield of material by considering its

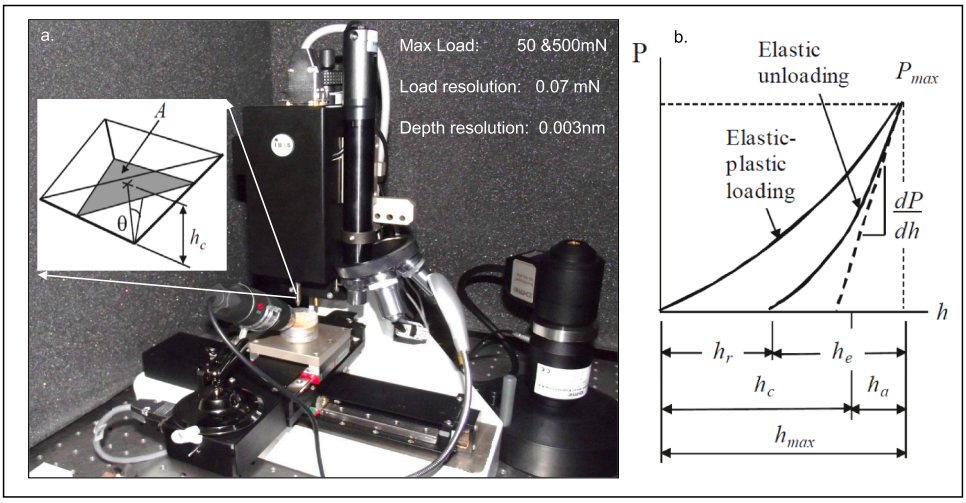

Fig. 1. The nano-indentation lab instrument used in this study shows the maximum load, depth resolution, and load resolution at Curtin University (a). The inset picture represents the Berkovich Indenter shape and parameters (not in scale). The nano-indentation load versus displacement curve is also presented for elastic-plastic loading, which is followed by elastic unloading (b). The parameters h_r, h_{max}, h_c, h_a are defined as the depth of the residual impression, the depth from the original specimen surface at the load P_{max}, the elastic displacement during unloading, and the distance from the edge of the contact to the specimen surface at full load, respectively. Upon elastic reloading, the tip of the indenter moves through a distance h_e, and the eventual point of contact with the specimen moves through a distance h_a. The method used in this study is based on the research conducted by Fischer-Cripps, 2007 in his work on Nano-indentation.

purely elastic unloading behavior. In this study, the indentation nano-scale modulus has been estimated using the following equation:

$$\frac{S}{M_0\sqrt{A_c}} = \frac{2}{\sqrt{\pi}}, \tag{5}$$

where the reduced or indentation modulus (M_0) reflects the overall elastic response of both the indenter and sample. To estimate the in-elastic indentation of an isotropic material, a relationship between M_0, Poisson's ratio and Young's modulus can be described as follows:

$$\frac{1}{M_0} = \frac{1-\nu^2}{E} + \frac{1-\nu_i^2}{E_i}, \tag{6}$$

In the above equation, ν is the Poisson's ratio of the studied sample, ν_i is the Poisson's ratio of the diamond indenter ($\nu_i = 0.07$), and E_i is Young's modulus of the diamond indenter ($E_i = 1140$ GPa). The Poisson's ratio of the studied samples is 0.28, as estimated from S-2. By rearranging Eq. (6), Young's modulus (E) of the studied samples can be estimated:

$$E = \left(1-\nu^2\right) \Big/ \left(\frac{1}{M_0} - \frac{1-\nu_i^2}{E_i}\right) \tag{7}$$

2.3. Fracture toughness

Fracture toughness measures a material's resistance to crack propagation under applied stress. It is a quantitative metric that is considered during rock characterization. The relationship between a material's mechanical properties and its fracture toughness is direct, where rigid and tough materials will have a lower tendency for the crack to propagate through them and vice-versa. To estimate the fracture toughness of a material, Liu et al. (2016) proposed an empirical linear equation based on Young's modulus. 20 tests were performed on four different samples from three members of the Bakken shale to define the relation. Considering the similarities between the studied samples and the Bakken shale, this study, directly used the relation to evaluate the fracture toughness of the samples. The equation is:

$$K_{IC} = 0.04048E + 0.7288 \tag{8}$$

The relation above shows a linear relationship between Young's Modulus (E) and fracture toughness, where an increase in E leads to an increase in fracture toughness. This relationship is supported by research, which has shown that an increase in Young's Modulus can lead to an increase in ultimate fracture strengths and improved resistance to fracture in rocks (Yuan and Xi, 2011).

3. Results

3.1. Nano-indentation curves analysis

The indentation moduli (M_0) of the samples were analyzed using the histogram to determine the distribution range and type of the values. The distribution of the samples is illustrated in Fig. 2, with samples from the same well grouped together. For example, samples S-2 & −3 from 32/4–1 are shown in Fig. 2b), while samples S-6, −7 & −8 from 34/4–3 are shown in Fig. 2e. Additionally, samples S-9, −10, −11 & −12 from well 15/3–8 are shown in Fig. 2f. The remaining samples are each represented by a single plot in Figs. 2a,c & d. To facilitate comparison, the same scale for M_0 is used in all plots. The average modulus values for each sample are also provided in parentheses.

A significant variation in values was observed, with the lowest value being estimated at 3.10 GPa in sample S-3 and the highest value being 38.10 GPa in sample S-4 (Fig. 2c). Despite this variation; the samples exhibit both normal and log-normal distribution. Some samples, such as S-4 (Fig. 2c) and S-6, −7&−8 (Fig. 2e), also exhibit multiple peaks in the histogram, indicating a mineral level property measurement. The distribution and average properties of the samples also varied significantly between samples from the same well (Figs. 2b, e & f).

3.2. Mineral composition and nanoscale properties

Generally, the mechanical property of any caprock shale is significantly dependent on mineral assemblages where clay-supported (higher clay particles) and grain-supported (silty and fewer clay minerals) shales represent considerable variation. Total organic carbon (TOC) also influenced the caprock shale to behave more ductile. In this section, the relationship between mineralogy and the nanoscale property has been evaluated. Nine out of twelve studied samples have available bulk X-ray diffraction (XRD) mineralogy, presented in Table 2 (Hansen et al., 2020; Rahman et al., 2020, 2022b). TOC of these samples was also estimated during the preparation of the XRD samples. In addition, the other

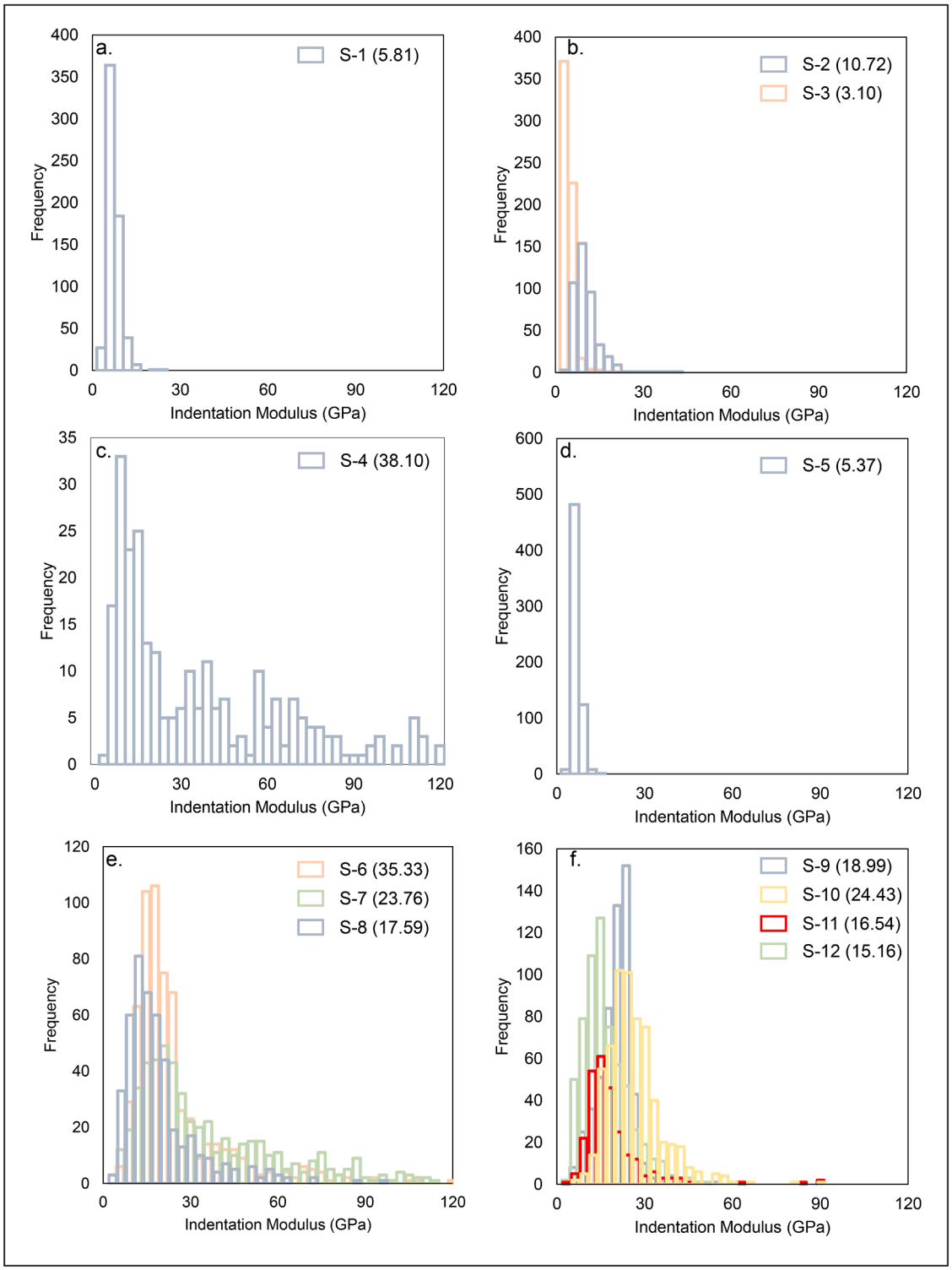

Fig. 2. The distribution of the indentation modulus (M_0) of studied samples represent the range and distribution type of each sample. Samples from the same well clustered in one plot. Moreover, the average M_0 is also shown within the plots.

mineral percentage in each well represents different fractions of carbonate (calcite, siderite, dolomite, ankerite), chloride (sylvite), and sulfates (barite, gypsum, alunite). The mineral percentage of these samples varied considerably. Based on the ductile mineral assemblages (i.e., Clay and TOC percentage), the studied samples have been divided into two clusters where S-1, −3, −5, −11, and −12 represent higher than 50 % of ductile minerals while S-4, −7, −9 and −10 have overall less than 50 %. Maximum ductile minerals are observed in S-1, while the minimum value is represented by sample S-4 (Table 2).

The relation between the indentation depth and the mechanical properties of the samples, such as hardness (H) and indentation modulus (M_0) can provide insight into the characteristics of the samples. Typically, during the initial stage of the nano-indentation test, the properties (i.e., H & M_0) depend on the surface stiffness of the sample. As the load increases, cracks begin to form, leading to decreased properties due to energy loss. This decrease is generally less severe than in the initial

stage. The behavior of the cracks, including their direction and length, is influenced by the samples' mineral composition and rock framework (Ping et al., 2015). The relation between H and M_0 with indentation depth is illustrated in Fig. 3 for samples with available bulk mineralogy analysis. With increasing load, a nonlinear negative correlation is observed between the strength properties and indentation depth. Shale samples show different shapes and the initial indentation depth breaking point compared within themselves. For instance, S-4 and −7 (Figs. 3c&e) have higher initial hardness and indentation modulus, but cracks generated and propagated quickly with a breaking point <1 μm indentation depth. S-10 and −11 (Figs. 3g&h) have similar breaking point (i.e., <1 μm), but initial property values are not as high, and the curve shape also differ considerably. The rest of the samples have very low initial values but have a gentle decrease with increasing load without having a sharp break (Figs. 3a, b,d,f&i).

Fig. 4 illustrates the linear relation between mineralogy and strength properties. Clay minerals indicated a negative correlation (decreasing with increasing property value) with rock strength properties (i.e., Young's modulus and hardness), while brittle minerals have a strong positive relationship. In addition, the correlation coefficient (R^2) of the studied plots explained that Young's modulus correlates better with mineralogy than rock hardness.

3.3. Sample type sensitivity

As rock's hardness and indentation modulus are intrinsic properties, those should not vary with different testing methods and sample types. To validate the effectiveness of cuttings as nano-indentation samples, four samples from the same well were analyzed. Cutting samples from drilling can be used in the nano-indentation method, which is an advantage in nanoscale laboratory property estimation. The sensitivity of the core and cutting samples in the nano-indentation technique has been evaluated using four samples (S-9 to −12) from well 15/3–8. S-9 and −12 are cutting samples, while S-10 and −11 are core samples (Table 1). Core samples illustrated a higher initial Young's modulus (E) value compared to the cutting samples (Fig. 5a). However, cracking generation with decreasing E with increasing indentation depth due to loading followed a similar trend. The average E value of the studied samples indicated that it did not have a large range. These samples' average hardness versus fracture toughness cross plot also indicated the minimum influence of type, such as cores or cuttings (Fig. 5b).

3.4. Load sensitivity

In the nano-indentation technique, different loads can be utilized during estimating mechanical properties. The sensitivity of load has been evaluated by comparing the output using 10 mN and 100 mN loads. The studied sample Young's modulus (E) varied when changing the applied load (Fig. 6a). However, changes are not significant and do not follow any trend. For instance, a few samples have a higher value in 10 mN load while others have the opposite trend. Linear relation between the applied loads indicated a considerably high correlation coefficient

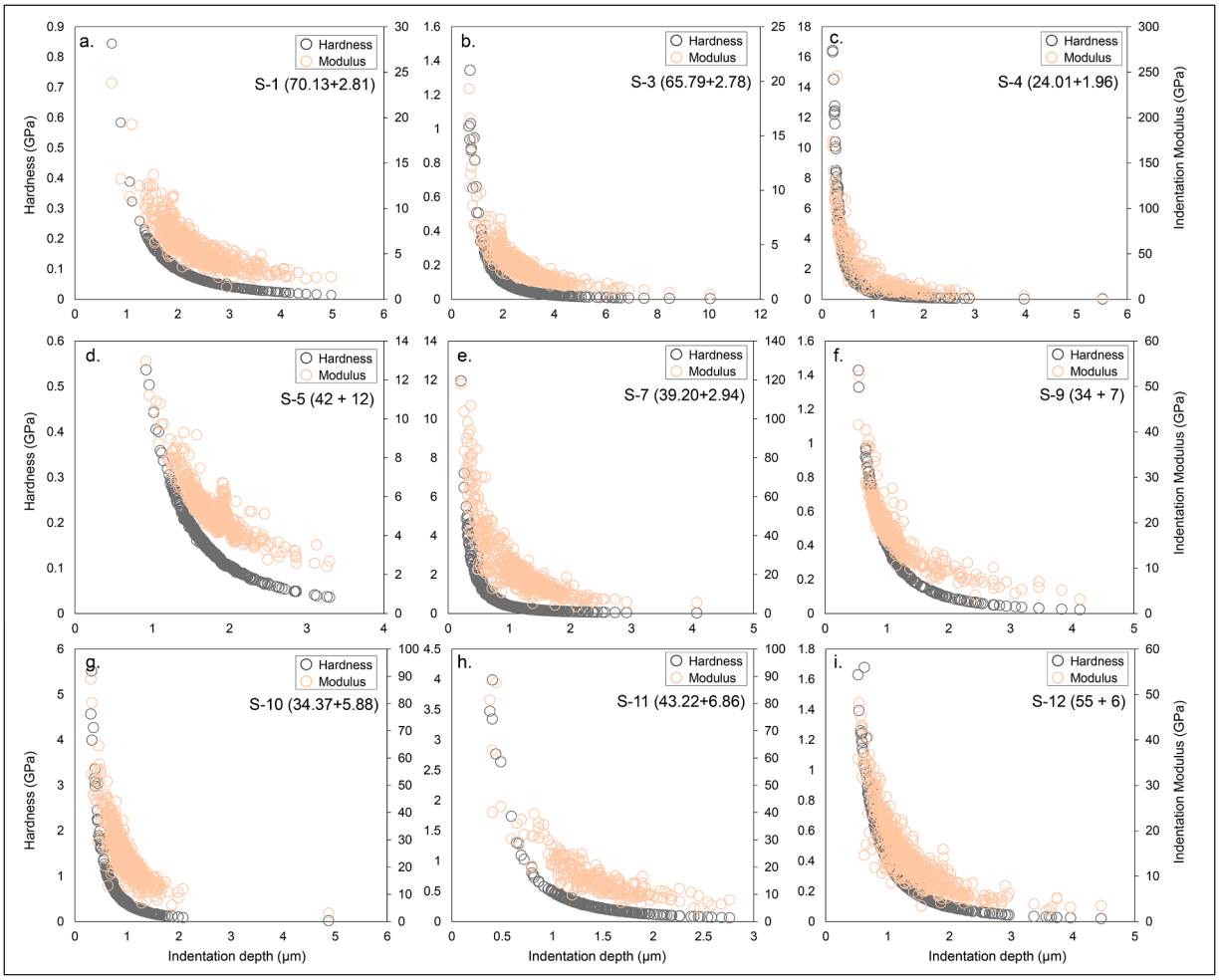

Fig. 3. The hardness and indentation modulus versus indentation depth was estimated in the nine samples with available XRD mineralogy data. The shape and value of the curves illustrated the strength of the rock. The value in the parenthesis indicated ductile mineral assemblages (Total clay + TOC) of that sample. Please note that the scales varied between the plots.

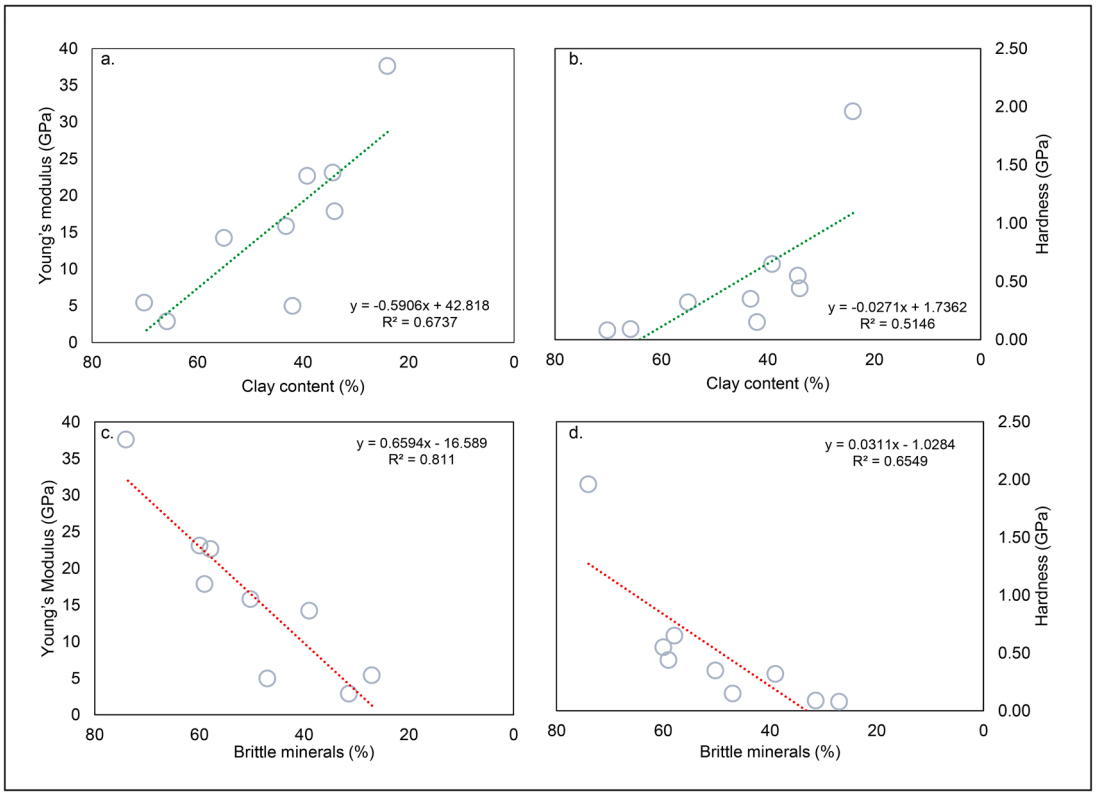

Fig. 4. Cross plots illustrate the strong relation between rock mineralogy and strength properties. The clay minerals percentage versus Young's modulus (a), and hardness (b) and Brittle mineral assemblages versus Young's modulus (c) and hardness (d) demonstrated a robust correlation by high R^2 values.

Table 1
Overview of the studied core and cutting samples show the paleo-depth and temperature.

Sample No.	Wells	Sample depth BSF (m)[a]	Paleo-depth BSF[a] (m)	Present temperature (°C)	Paleo-temperature[a] (°C)	Sample type
S-1	32/2–1	502	1302	15.23	39.50	Cuttings
S-2	32/4–1	804	1504	29.62	55.41	Cuttings
S-3	32/4–1	825	1525	30.39	56.18	Cuttings
S-4	35/11–4	1609	1799	56.64	63.33	Core
S-5	15/12–21	2777	2777	97.19	97.19	Cuttings
S-6	34/4–3	3179	3179	95.38	95.38	Core
S-7	34/4–3	3188	3188	95.65	95.65	Core
S-8	34/4–3	3193	3193	95.79	95.79	Core
S-9	15/3–8	3924	3924	123.16	123.16	Cuttings
S-10	15/3–8	4056	4056	127.33	127.33	Core
S-11	15/3–8	4071	4071	127.78	127.78	Core
S-12	15/3–8	4317	4317	135.49	135.49	Cuttings

[a] Exhumation corrected.

Table 2
Bulk XRD mineralogy of the study samples.

Sample No.	Quartz (%)	Feldspar (%)	Pyrite (%)	Clay minerals (%)	TOC (%)	Others (%)
S-1	17.71	4.06	0.55	70.13	2.81	4.74
S-3	24.65	0.00	1.76	65.79	2.78	5.02
S-4	35.92	4.88	18.17	24.01	1.96	15.06
S-5	30.00	0.00	9.00	42.00	12.00	8.00
S-7	24.00	27.65	2.72	39.20	2.94	3.52
S-9	54.00	0.00	5.00	34.00	7.00	0.00
S-10	51.56	0.00	7.12	34.37	5.88	1.28
S-11	42.90	0.00	7.34	43.22	6.86	0.00
S-12	31.00	0.00	8.00	55.00	6.00	0.00

(R^2~0.88) value (Fig. 6b).

3.5. Fracture toughness

The relation of fracture toughness with hardness and total clay content is presented in Fig. 7. The fracture toughness values of the study samples ranged between 0.85 and 2.25 GPa. The studied samples illustrated a strong positive linear relation with hardness (Fig. 7a). On the contrary, a higher negative correlation is observed with total clay (Fig. 7b). With increasing bulk clay mineralogy, fracture toughness decreases linearly.

3.6. Comparative analysis

A comparative analysis of Young's modulus (E) between conventional triaxial laboratory tests and nano-indentation techniques has been carried out using the scouted database from Horsrud et al. (1998) and

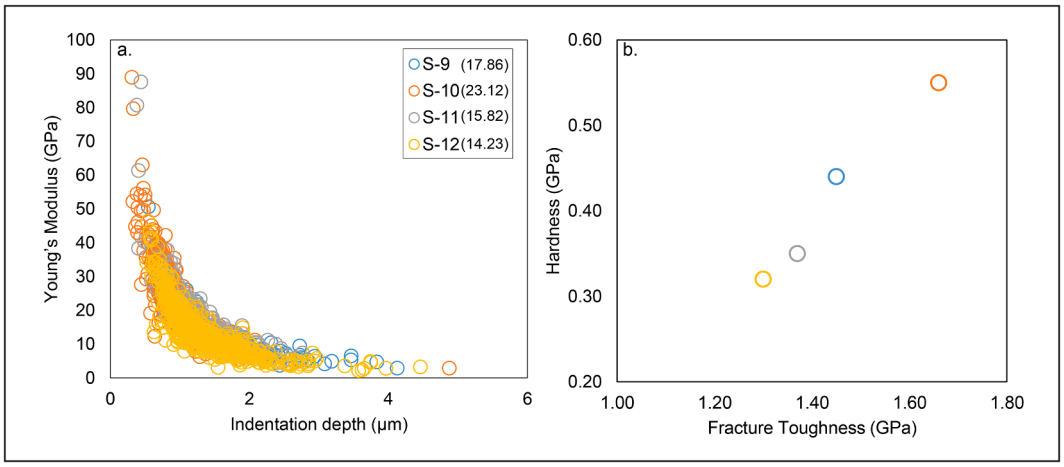

Fig. 5. The sensitivity of core and cuttings samples on rock strength properties are illustrated by showing the four studied samples from the same well. The nanoscale estimated Young's modulus is plotted against the indentation depth (a) while the average hardness versus Fracture toughness is presented (b). Note that the parenthesis value indicated the average Young's modulus of that sample.

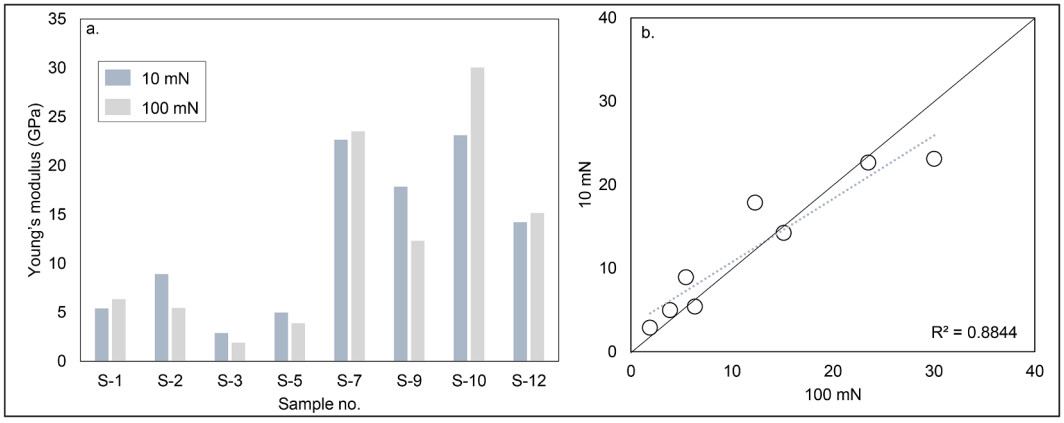

Fig. 6. The average nanoscale estimated Young's modulus in different samples is compared with 10 mN, and 100 mN applied loads (a). The cross plot of the same database shows a robust correlation between both loads (b).

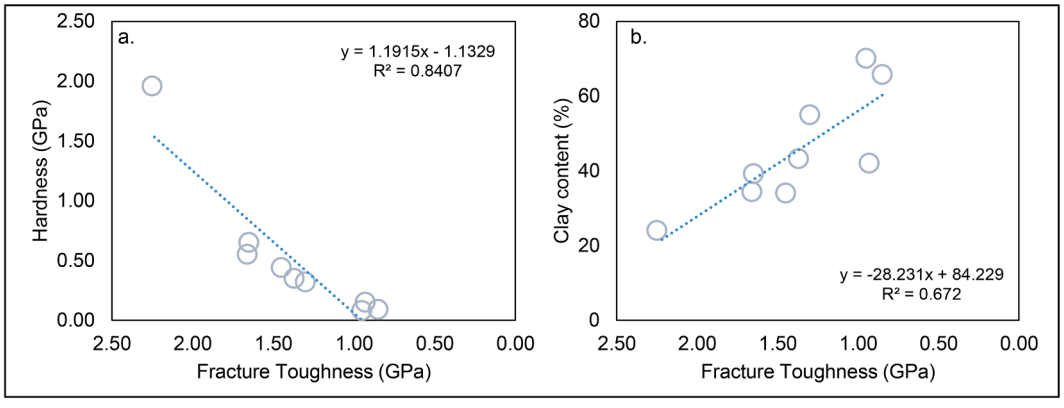

Fig. 7. The fracture toughness estimated using Young's modulus is correlated with the hardness (a) and bulk clay minerals (b).

the studied samples, respectively. Data points have been plotted in Young's modulus versus bulk clay mineralogy cross plot (Fig. 8a). Nanoscale property negatively relates to bulk mineralogy where E increases with decreasing the bulk clay percentage. A linear correlation coefficient is also high, about 66 %. Triaxial lab properties, however, do not follow any relation with bulk clay, instead having a lower E value except for the deeper sample located at 4870 m depth (Fig. 8b). Overall, triaxial lab measurement represented a lower E value compared with the average nanoscale property. All the data points (triaxial and nano-intended) have been clustered into two zones in depth versus Young's modulus plot, excluding one outlier where <3000 m depth samples represent lower E compared to >3000 m depth sample (Fig. 8b). Within the deeper cluster, the nanoscale property has higher values with a large range compared to the single triaxial data point.

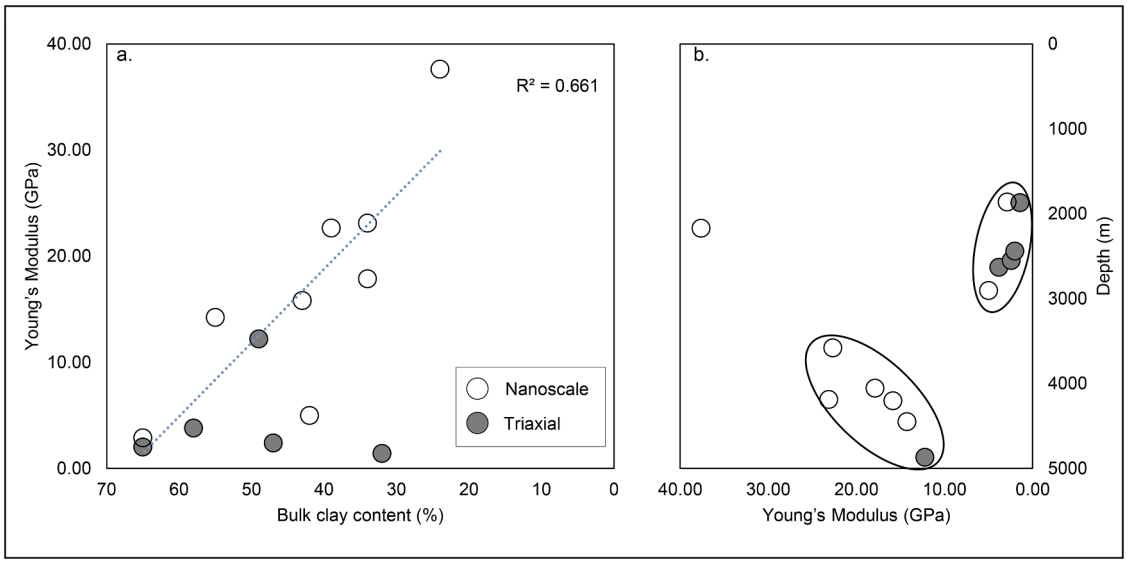

Fig. 8. The triaxial lab result (Horsrud et al., 1998) and nanoscale (this study) Young's modulus are plotted with bulk clay mineralogy (a) and depth (b) for comparison. Nanoscale Young's modulus negatively affects bulk clay mineralogy with a correlation coefficient of 0.66.

4. Discussion

The mineralogy of the caprock has a significant impact on its nanoscale properties (Fig. 4). Ductile mineral assemblages (i.e., Total clay and TOC) have been found to affect the behavior of the samples under load. Samples with higher ductile mineral content exhibit low initial values, but as the load increases, instead of cracking, these ductile minerals absorb additional stress and show a gentle decrease in the curve without generating or propagating cracks (Fig. 3). In contrast, samples with higher brittle mineral content have high initial value but crack quickly with a sharp breaking point.

Fracture toughness (FT) values also show a strong negative correlation with clay mineralogy (Fig. 7). Although higher FT represents greater resistance to crack initiation, the rock becomes more brittle with sharp breaking points under applied load. Regarding top seal integrity, it is important to balance the toughness and brittleness of the caprock shales to withstand reservoir pressure from below.

Relatively shallow depth but highest modulus value sample S-4 has abundant pyrite and siltier (coarser grain relative to clayey samples) with a lower percentage of ductile mineral assemblages (Rahman et al., 2021, 2020). SEM images of S-4 are illustrated in Fig. 9. Several indentation moduli pick samples such as S-4, −6, −7 & −8 (Figs. 2c&e) explained the mineral level property estimations in the nano-indentation technique. Several stronger minerals also added up with a higher average modulus, indicating relatively brittle caprocks.

Additionally, the shape and value of the indentation modulus in relation to indentation depth are strongly influenced by rock minerals regardless of different diagenesis levels. Although a specific ductile mineral assemblage cutoff cannot be determined due to the limited number of samples, values above 50 % are considered to be a reasonable threshold for distinguishing between brittle and ductile caprocks. Additionally, high TOC with maturation may lead to maturation-induced micro-fractures, which can influence indentation stress distribution.

The use of the nano-indentation technique to evaluate the mechanical properties of rock has been growing in popularity in recent years due to its reliability and simplicity (Abedi et al., 2016; Charlton et al., 2021; Du et al., 2020; Ping et al., 2015). This study has also shown that the results obtained using this method are comparable to those obtained using conventional triaxial laboratory tests on samples from the same basin. Fig. 10 shows the correlation between the results obtained in this study and published data, and a good agreement was observed. This confirms the reliability of nano-indentation methods for rock strength characterization.

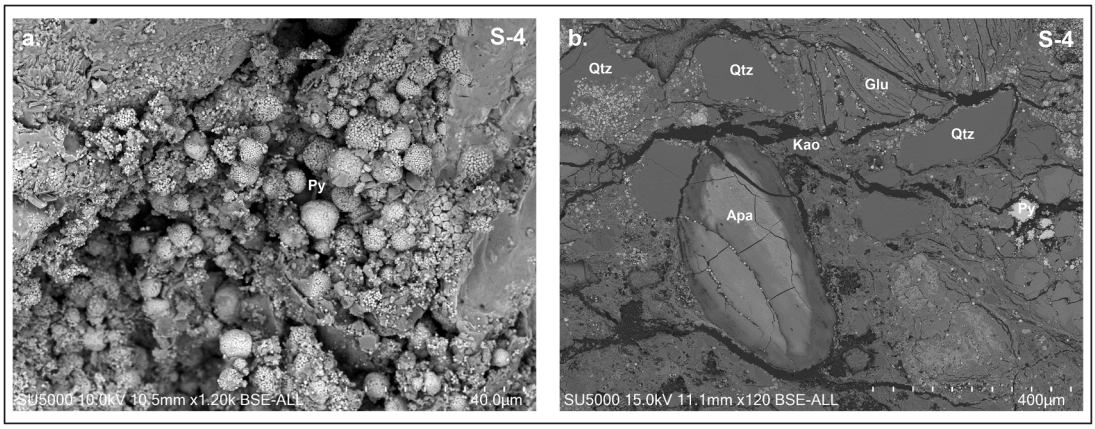

Fig. 9. The SEM images of S-4 show the microscopic illustration of grain size, mineral types (Qtz-Quartz; Glu-Gluconite; Kao-Kaolinite; Apa-Apatite; Py-Pyrite; Plag-Plagioclase; Cal-Calcite; OM-Organic Matter). Please note that the scale varied between images.

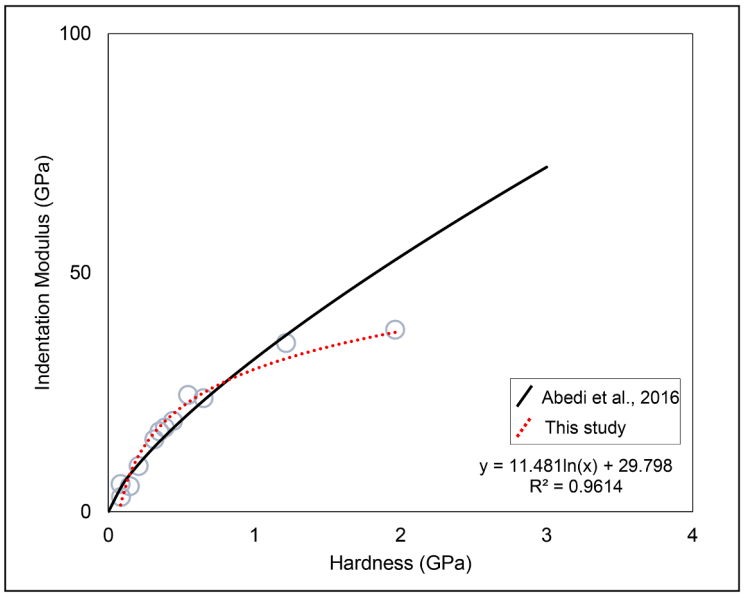

Fig. 10. The indentation modulus versus hardness cross pot of the studied samples compared to the published clay/kerogen-rich rock samples proposed by Abedi et al. (2016).

4.1. Implications

Geomechanical modeling is a powerful tool for understanding the behavior of subsurface rock formations under different stress scenarios. This technique can be used to predict the behavior of overburden, caprock, and reservoir rock in carbon capture and storage (CCS) projects and to predict the behavior of rock formations that may contain hydrocarbons in hydrocarbon exploration and production. By simulating subsurface conditions, geomechanical models can help optimize the design and operation of these projects and identify the most favorable production strategies.

Rock strength properties, such as Young's modulus, hardness, and fracture toughness, are important input parameters in geomechanical simulation. These properties affect the stress and strain distribution in the subsurface, which in turn influences the stability of reservoirs, cap and overburden rocks, and the potential for fluid leakage. Accurate estimates of rock strength properties are essential for reliable predictions of subsurface behavior. Therefore, it is crucial to have accurate rock strength properties to evaluate the feasibility and risks of subsurface operations such as CCS and hydrocarbon exploration and production. However, conventional laboratory measurements are scarce due to the lack of cores within the cap and overburden.

The nano-indentation can be an alternative laboratory measurement technique. This study has proven the reliability and accuracy of the estimated properties, such as hardness and indentation modulus. Additionally, nano-indentation can be performed on small cutting samples, making it a useful alternative to conventional laboratory testing for overburden rocks where very few or no cores are available. This can help to reduce data scarcity within the cap and overburden intervals and improve the accuracy of geomechanical models for CCS and hydrocarbon exploration and production.

5. Conclusions

The key outcomes from this study are as follows:

- The shape and frequency of the studied samples indentation moduli histograms vary considerably, where few samples illustrate multiple peaks indicating mineral level estimation.
- Nanoscale properties are significantly influenced by rock mineralogy. The organic-rich caprock shale samples have a positive correlation with ductile minerals, while a strong negative relation is observed with brittle mineral assemblages.
- Due to the intrinsic behavior of rock, cuttings can be effectively used in mechanical property estimation.
- The maximum applied load has minimal influence on nanoscale property.
- Both nano-indentation and triaxial lab measurement results from caprock shale are comparable.

We can conclude that the nano-indentation method in organic-rich caprock shales mechanical property estimation using cutting samples is reliable. This finding will add significant value in field-scale geomechanical modeling for CCS and hydrocarbon exploration and production.

CRediT authorship contribution statement

Md Jamilur Rahman: Conceptualization, Formal analysis, Investigation, Methodology, Software, Validation, Visualization, Writing – original draft, Writing – review & editing. **Maxim Lebedev:** Formal analysis, Validation, Writing – review & editing. **Nazmul Haque Mondol:** Funding acquisition, Project administration, Supervision, Validation, Writing – review & editing.

Declaration of competing interest

The authors declare that they have no known competing financial interests or personal relationships that could have appeared to influence the work reported in this paper

Data availability

Data will be made available on request.

Acknowledgements

We are thankful for the funding provided by the Research Council of

Norway for the OASIS (Overburden Analysis and Seal Integrity Study for CO_2 Sequestration in the North Sea) project (NFR-CLIMIT project #280472). We are indebted to the additional funding provided by Equinor and TotalEnergies. We are also grateful for the studied samples provided by Norwegian Petroleum Directorate (NPD) and Gassnova.

References

Abedi, S., Slim, M., Ulm, F.J., 2016. Nanomechanics of organic-rich shales: the role of thermal maturity and organic matter content on texture. Acta Geotech. 11, 775–787.
Amann-Hildenbrand, A., Ghanizadeh, A., Krooss, B.M., 2012. Transport properties of unconventional gas systems. Mar. Pet. Geol. 31, 90–99.
Bulychev, S.I., Alekhin, V.P., Shorshorov, M.K., Ternovskij, A.P., Shnyrev, G.D., 1975. Determination of young modulus by the hardness indentation diagram. Zavodskaya Lab. 41 (9), 1137–1140.
Charlton, T.S., Goodarzi, M., Rouainia, M., Aplin, A.C., Cubillas, P., 2021. Effect of diagenesis on geomechanical properties of organic-rich calcareous shale: a multiscale investigation. J. Geophys. Res. Solid Earth 126 e2020JB021365.
Colmenares, L.B., Zoback, M.D., 2002. A statistical evaluation of intact rock failure criteria constrained by polyaxial test data for five different rocks. Int. J. Rock Mech. Min. Sci. 39, 695–729.
Du, J., Whittle, A.J., Hu, L., Divoux, T., Meegoda, J.N., 2020. Characterization of meso-scale mechanical properties of Longmaxi shale using grid microindentation experiments. J. Rock Mech. Geotech. Eng.
Fawad, M., Rahman, M.J., Mondol, N.H., 2021. Seismic reservoir characterization of potential CO_2 storage reservoir sandstones in Smeaheia area, Northern North Sea. J. Pet. Sci. Eng. 205, 108812.
Fawad, M., Rahman, M.J., Mondol, N.H., 2020. Seismic-derived geomechanical properties of potential CO_2 storage reservoir and caprock in Smeaheia area, northern north sea - submitted for review. Lead. Edge.
Fischer-Cripps, A.C., 2007. Introduction to contact Mechanics, 2nd ed. Springer-Verlag, New York. https://doi.org/10.1007/978-0-387-68188-7.
Foschi, M., Cartwright, J.A., 2020. Seal failure assessment of a major gas field via integration of seal properties and leakage phenomena. Am. Assoc. Pet. Geol. Bull. 104, 1627–1648.
Hansen, J.A., Mondol, N.H., Tsikalas, F., Faleide, J.I., 2020. Caprock characterization of upper jurassic organic-rich shales using acoustic properties, norwegian continental shelf. Mar. Pet. Geol. 121, 104603 https://doi.org/10.1016/j.marpetgeo.2020.104603.
Hart, B.S., Macquaker, J.H.S., Taylor, K.G., 2013. Mudstone ("shale") depositional and diagenetic processes: implications for seismic analyses of source-rock reservoirs. Interpretation 1, B7–B26.
Hongyan, W., Yuzhang, L., Dazhong, D., Qun, Z., Dong, D., 2013. Scientific issues on effective development of marine shale gas in southern China. Pet. Explor. Dev. 40, 615–620.
Horsrud, P., Sønstebø, E.F., Bøe, R., 1998. Mechanical and petrophysical properties of north sea shales. Int. J. Rock Mech. Min. Sci. 35, 1009–1020.
Hu, Q., Ewing, R.P., Dultz, S., 2012. Low pore connectivity in natural rock. J. Contam. Hydrol. 133, 76–83.
Ingram, G.M., Urai, J.L., Naylor, M.A., 1997. Sealing processes and top seal assessment. in: Norwegian Petroleum Society Special Publications. Elsevier, pp. 165–174.
Lama, R.D., Vutukuri, V.S., 1978. Handbook on mechanical properties of rocks-testing techniques and results-volume III. ISBN: 0-87849-021-3.
Li, Y., Yang, J., Pan, Z., Tong, W., 2020. Nanoscale pore structure and mechanical property analysis of coal: an insight combining AFM and SEM images. Fuel 260, 116352.
Mehmani, A., Prodanović, M., Javadpour, F., 2013. Multiscale, multiphysics network modeling of shale matrix gas flows. Transp. porous media 99, 377–390.
Minaeian, V., Rasouli, V., Dewhurst, D., 2014. A laboratory procedure proposed for mechanical testing of shales. APPEA J 54, 337–344.
Mondol, N.H., 2018. Seal quality prediction using e-poisson's ratio rock physics templet – a case study from the norwegian Barents sea. Geoconvention-2018, May 7-11, Calgary, Canada.
Mondol, N.H., Bjørlykke, K., Jahren, J., 2008. Experimental compaction of clays: relationship between permeability and petrophysical properties in mudstones. Pet. Geosci. 14, 319–337.
Mondol, N.H., Bjørlykke, K., Jahren, J., Høeg, K., 2007. Experimental mechanical compaction of clay mineral aggregates—changes in physical properties of mudstones during burial. Mar. Pet. Geol. 24, 289–311.
Oliver, W.C., Pharr, G.M., 2004. Measurement of hardness and elastic modulus by instrumented indentation: advances in understanding and refinements to methodology. J. Mater. Res. 19, 3–20.
Oliver, W.C., Pharr, G.M., 1992. An improved technique for determining hardness and elastic modulus using load and displacement sensing indentation experiments. J. Mater. Res. 7, 1564–1583.
Ping, C., Qiang, H.A.N., Tianshou, M.A., Dong, L.I.N., 2015. The mechanical properties of shale based on micro-indentation test. Pet. Explor. Dev. 42, 723–732.
Rahman, M.J., Fawad, M., Choi, J.C., Mondol, N.H., 2022a. Effect of overburden spatial variability on field-scale geomechanical modeling of potential CO_2 storage site Smeaheia, offshore Norway. J. Nat. Gas Sci. Eng. 99, 104453.
Rahman, M.J., Fawad, M., Jahren, J., Mondol, N.H., 2022b. Top seal assessment of drake formation shales for Co2 storage in the horda platform area, offshore Norway. Int. J. Greenh. Gas Control Revised ve.
Rahman, M.J., Fawad, M., Mondol, N.H., 2022c. 3D Field-scale geomechanical modeling of potential CO_2 storage site smeaheia. Offshore Norway. Energies 15. https://doi.org/10.3390/en15041407.
Rahman, M.J., Fawad, M., Mondol, N.H., 2020. Organic-rich shale caprock properties of potential CO_2 storage sites in the northern north sea, offshore Norway. Mar. Pet. Geol. 122, 104665.
Rahman, M.J., Lebedev, M., Mondol, N.H., 2021. Nanoscale mechanical properties of organic-rich draupne shale caprock, offshore Norway. In: in: SEG/AAPG/SEPM First International Meeting for Applied Geoscience & Energy. OnePetro.
Rickman, R., Mullen, M.J., Petre, J.E., Grieser, W.V., Kundert, D., 2008. A practical use of shale petrophysics for stimulation design optimization: all shale plays are not clones of the Barnett Shale. In: in: SPE Annual Technical Conference and Exhibition. Society of Petroleum Engineers.
Sakhaee-Pour, A., Bryant, S.L., 2012. Gas permeability of shale. SPE Reserv. Eval. Eng. 15, 401–409.
Schowalter, T.T., 1979. Mechanics of secondary hydrocarbon migration and entrapment. Am. Assoc. Pet. Geol. Bull. 63, 723–760.
Sone, H., Zoback, M.D., 2013a. Mechanical properties of shale-gas reservoir rocks—Part 1: static and dynamic elastic properties and anisotropy. Geophysics 78, D381–D392.
Sone, H., Zoback, M.D., 2013b. Mechanical properties of shale-gas reservoir rocks—Part 2: ductile creep, brittle strength, and their relation to the elastic modulus. Geophysics 78, D393–D402.
Storvoll, V., Bjørlykke, K., Mondol, N.H., 2005. Velocity-depth trends in mesozoic and cenozoic sediments from the norwegian shelf. Am. Assoc. Pet. Geol. Bull. 89, 359–381.
Tianshou, M.A., Ping, C., 2014. Study of meso-damage characteristics of shale hydration based on CT scanning technology. Pet. Explor. Dev. 41, 249–256.
Vernik, L., Milovac, J., 2011. Rock physics of organic shales. Lead. Edge 30, 318–323.
Wang, Z., 2002. Seismic anisotropy in sedimentary rocks, part 2: laboratory data. Geophysics 67, 1423–1440.
Xiong, J., Liu, K., Liang, L., Liu, X., Zhang, C., 2019. Investigation of influence factors of the fracture toughness of shale: a case study of the Longmaxi formation shale in Sichuan Basin. China. Geotech. Geol. Eng. 37, 2927–2934.
Yuan, C.C., Xi, X.K., 2011. On the correlation of Young's modulus and the fracture strength of metallic glasses. J. Appl. Phys. 109, 33515.
Zhang, P., Hu, L., Meegoda, J.N., 2017. Pore-scale simulation and sensitivity analysis of apparent gas permeability in shale matrix. Materials. (Basel) 10, 104.
Zhang, Pengwei, Hu, L., Meegoda, J.N., Gao, S., 2015a. Micro/nano-pore network analysis of gas flow in shale matrix. Sci. Rep. 5, 1–11.
Zhang, P., Hu, L., Wen, Q., Meegoda, J.N., 2015b. A multi-flow regimes model for simulating gas transport in shale matrix. Géotechnique Lett 5, 231–235.
Zuo, J.P., Li, Y.L., Liu, C., Liu, H., Wang, J., Li, H., Liu, L., 2019. Meso-fracture mechanism and its fracture toughness analysis of Longmaxi shale including different angles by means of M-SENB tests. Eng. Fract. Mech. 215, 178–192.
Zuo, J., Lu, J., Ghandriz, R., Wang, J., Li, Y., Zhang, X., Li, J., Li, H., 2020. Mesoscale fracture behavior of Longmaxi outcrop shale with different bedding angles: experimental and numerical investigations. J. Rock Mech. Geotech. Eng. 12, 297–309.